

Supplement of The Cryosphere Discuss., 8, 3237–3261, 2014
<http://www.the-cryosphere-discuss.net/8/3237/2014/>
doi:10.5194/tcd-8-3237-2014-supplement
© Author(s) 2014. CC Attribution 3.0 License.



Supplement of

Detailed ice loss pattern in the northern Antarctic Peninsula: widespread decline driven by ice front retreats

T. A. Scambos et al.

Correspondence to: T. A. Scambos (teds@nsidc.edu)

Section S1 – Summary of satellite image data

The satellite imagery used in dDEMs across the northern Antarctic Peninsula is identified in Table S1 and the spatial extents are indicated in Figure S1.

Section S2 – Tabular results for 33 glacier basins in the nAP

This section contains supporting text for the full study results for all the Antarctic Peninsula glacial basins and islands <66°S. Table S2 presents the full analysis of all 33 major glacial basins and 9 sub-basins in the study region, including area, estimated mass change rates, volume change rates, and percentage extent of measurement relative to full basin area. To assess the mass input and estimated net imbalance of the glacier basins in the nAP, we calculated the total mass input provided by the RACMO-2 climate model for each of the basins and their associated elevation bin regions. This section includes Table S3 that compares the total mass balance (dM/dt) and input surface mass (dMi/dt), and resulting imbalance ratio for each basin.

Section S3 – Comparison of ICESat and dDEM dh/dt measurements and bias analysis

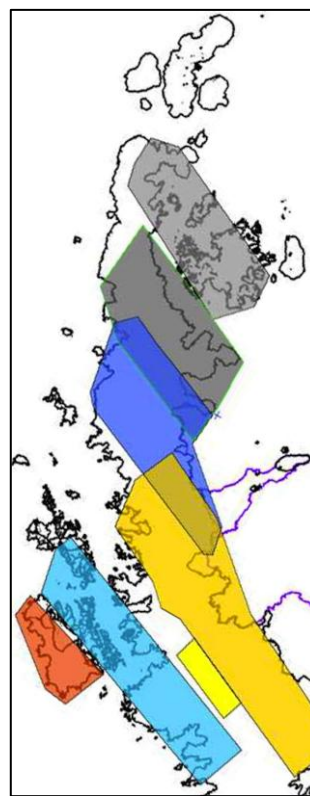
This section includes supporting text and tables that summarizes our error and bias analyses. By extracting dh/dt at the same location from both the ICESat repeat-track analysis (slope-corrected dh/dtICESat) and the difference DEM analysis (dh/dt dDEM) we examined biases and potential errors in dh/dt. This analysis is summarized in Table S3 for co-located dDEM and ICESat data. This section also includes an analysis of ICESat ascending versus descending track crossovers before and after slope corrections were applied (see Table S4). The overall dh/dt error assessment shows small differences in dh/dt between the two methods, with consistent agreement over areas varying in mean elevation, latitude, and mean rate of elevation change. Therefore, we conclude that the two methods may be used together without a bias adjustment. Further, we conducted a bias analysis of the dDEMs. For each basin, the differences shown in Table S4 [dh/dtdDEM - dh/dtICESat] can be compared to the median of dh/dtdDEM on nunataks, where no elevation change is expected (a version of the ‘null’ test) and these results are summarized in Figures S2, S3, and S4.

Section S4 – References

References used within the Supplementary Information sections are listed here.

Table S1 and Figure S1. Summary of satellite image data
Satellite stereo-imagery used in dDEMs across the northern Antarctic Peninsula.

Region (Fig. A1 colour)	Date	Satellite	Sensor	Image ID
Southwest (orange and light blue)	21 Dec. 2004	TERRA	ASTER	AST_L1A.003:2027139564
	06 Dec. 2005	TERRA	ASTER	AST_L1A.003:2032166777
	05 Dec. 2010	SPOT5	HRS	GES 11-032
James Ross Is. (light gray)	08 Jan. 2001	TERRA	ASTER	AST_L1A.003:2004102905
	23 Jan. 2006	SPOT5	HRS	GES 08-025
Sjögren/PGC (dark gray)	26 Sep. 2001	TERRA	ASTER	AST_L1A.003:2004337049
	07 Jan. 2006	SPOT5	HRS	SPI 09-047
Larsen A (dark blue)	02 Oct. 2003	TERRA	ASTER	AST_L1A.003:2017716438
	17 Nov. 2008	SPOT5	HRS	GES 12-032
Larsen B (gold/yellow)	22 Nov. 2001	TERRA	ASTER	AST_L1A.003:2005067298
	07 Nov. 2002	TERRA	ASTER	AST_L1A.003:2009058253
	25 Nov. 2006	SPOT5	HRS	GES 08-037



ASTER: Advanced Spaceborne Thermal Emission and Reflection Radiometer;
SPOT5: Satellite Pour l'Observation de la Terre.
HRS: Haute Résolution Stéréoscopique.

SPOT5–HRS product image identification code corresponds to the SPIRIT database². When multiple images from an ASTER strip have been used, the image identification of the northernmost image is given.

Section S2. Full Results for Antarctic Peninsula glacial basins and islands <66°S

Table S2 presents the full analysis of all 33 major glacial basins and 9 sub-basins in the study region, including area, estimated mass change rates, volume change rates, and percentage extent of measurement relative to full basin area for difference DEMs (hereafter dDEMs), or the number of ICESat-derived along-track elevation change measurements within the basin. Basin numbers are shown in Figure S1 and Tables S1 and S5. The results are also presented as combined regions, at the top of the tables (S1 and S5) as sets of selected eastern coast outlets, western coast outlets, and the entire nAP study area. Results are also separated into elevation zones (above or below 1000 m a.s.l.). Below 1000 m a.s.l., measurements of volume change are determined by a combination of dDEM results and cross-track slope-adjusted ICESat repeat-track results. A hypsometric interpolation of the available elevation change rate data (dH/dt) is used to infill unmeasured areas. To allow the small number of ICESat-based dH/dt measurements to influence the hypsometric averaging with the typically much larger number of dDEM dH/dt pixels, the ICESat dH/dt measurements were weighted by 10 (i.e. equivalent to 10 50 x 50 m dDEM grid cells). This was important in regions where only a small percentage of the elevation band (perhaps a non-representative percentage) was measured by the dDEM method. Above 1000 m a.s.l., elevation change measurements are a simple average of ICESat-determined dH/dt measurements only, due to the sparseness and likely lower reliability of the dDEM data in smooth high-elevation areas. Although not used in the final elevation change and mass change estimates, Figure 1 (main text) shows the dDEM coverage above 1000 m, and the majority of it is valid data.

Table S2. Mass balance and volume change estimates for glaciers and sub-regions of the northern Antarctic Peninsula from combined satellite stereo-image and altimetry analysis. Units: Area (km²), Mean dM/dt (Gt a⁻¹), Number of Measurements, Mean dH/dt (m a⁻¹), Mean dV/dt (km³ a⁻¹)

Region	Ice-CoveredTotal					Ice Front Retreat					Below 1000 m a.s.l.					Above 1000 m a.s.l.			
	Area	dM/dt ^a	Area ^b	dH/dt ^c	dV/dt ^{d,h}	Area	dDEM ^e	ICESat ^f	dH/dt ^g	dV/dt ^h	Area	ICESat ^f	dH/dt ^g	dV/dt ^h					
nAP <66°S, 1-33	34232.8	-24.9	325.6	-3.5	-1.2	23096.5	44.8	12476	-1.00	-23.1	10651.7	2668	-0.31	-3.4					
nAP West, 1-11	14338.2	-4.8	7.8	-5.3	-0.2	9014.5	38.6	2999	-0.27	-2.4	5323.7	893	-0.59	-2.8					
nAP North, 12-14	3688.0	-2.4	4.0	-3.3	-0.1	3684.3	8.2	2204	-0.69	-2.5	3.7	(0)	(-0.31)	0.0					
nAP East, 15-33	16207.5	-17.7	313.8	-5.7	-0.9	10884.0	62.4	7279	-1.67	-18.2	5323.5	1775	-0.14	-0.6					
1 Bigo-Barilari B. 1a Cadman Gl.	1737.4 309.6	-1.37 -0.37	2.7 2.7	-3.8 -3.8	-0.01 -0.01	825.4 101.4	38.6 53.8	210 97	-0.88 -2.23	-0.72 -0.23	912.0 208.2	152 (0)	-0.88 (-0.88)	-0.80 -0.18					
2 Trooz-Lever Gl.	1479.7	0.50	--	--	--	771.5	71.5	425	0.72	0.56	708.3	(19)	-0.31	-0.22					
3 Flandres B.	1123.7	-0.45	--	--	--	403.8	57.8	156	-0.14	-0.06	720.0	60	-0.61	-0.44					
4 Anvers Is. 4a Ricke B.	2155.9 83.3	-0.33 -0.21	3.0 3.0	-6.0 -6.0	-0.01 -0.01	1965.2 83.3	40.4 44.5	844 120	-0.16 -2.71	-0.32 -0.23	191.7 --	(0)	(-0.31)	-0.05 --					
5 Andvord B.	1163.2	-0.19	--	--	--	641.6	23.9	80	-0.06	-0.04	521.5	85	-0.33	-0.17					
6 Brabant Is. 6a Rush Gl.	916.7 43.6	-0.43 -0.07	2.1 2.1	-6.2 -6.2	-0.01 -0.01	672.4 28.2	28.7 96.3	14 3	-0.61 -2.64	-0.41 -0.08	244.4 14.7	(2) (0)	(-0.31) (-0.31)	-0.07 -0.00					
7 Charlotte B.	505.5	-0.50	--	--	--	316.7	13.6	(0)	-1.57	-0.50	188.8	(0)	(-0.31)	-0.05					
8 Cayley Gl.	1512.6	-0.75	--	--	--	817.4	28.1	255	-0.81	-0.66	695.2	221	-0.25	-0.17					
9 Wright Ice Pied.	1370.1	-1.22	--	--	--	845.6	57.8	314	-1.35	-1.14	524.3	209	-0.40	-0.21					
10 Charcot B.	800.9	-0.37	--	--	--	437.2	57.9	159	0.14	0.06	363.7	140	-1.30	-0.47					
11 West Trinity	1571.5	0.68	--	--	--	1317.7	17.1	542	0.63	0.83	253.8	(5)	(-0.31)	-0.08					
12 Mott Snowfield 12a North Duse B.	987.7 242.9	-1.12 -0.45	4.0 4.0	-3.3 -3.3	-0.01 -0.01	984.0 239.2	14.6 17.7	536 230	-1.26 -2.04	-1.24 -0.49	3.7 3.6	(0) (0)	(-0.31) (-0.31)	0.00 0.00					
13 Tabarin Pen.	363.9	-0.65	--	--	--	363.9	43.8	140	-1.98	-0.72	--	--	--	--					
14 Joinville-Du.-D'U. Is.	2336.4	-0.53	--	--	--	2336.4	0.0	1528	-0.25	-0.58 ⁱ	0.0	--	--	--					
15 Vega Is.	175.7	-0.25	--	--	--	175.7	70.1	34	-1.58	-0.28	0.0	--	--	--					
16 Snow Hill Is.	312.5	-0.27	--	--	--	312.5	0.0	163	-0.96	-0.30 ⁱ	0.0	--	--	--					
17 North JRI	524.6	-0.64	--	--	--	389.6	37.2	70	-2.00	-0.78	134.9	96	0.05	0.07					
18 South JRI	568.5	-0.24	8.1	-1.1	-0.00	364.8	60.3	169	-0.78	-0.29	203.7	119	0.13	0.03					
19 West JRI	707.7	-1.52	39.0	-3.8	-0.07	625.6	69.4	178	-2.56	-1.60	82.1	(0)	(-0.31)	-0.02					
20 East Trinity	1347.0	0.55	--	--	--	1119.2	64.0	850	0.67	0.75	227.8	(0)	(-0.31)	-0.06					
21 Sjögren Gl.	1177.3	-1.16	19.2	-3.0	-0.03	852.8	81.9	297	-1.64	-1.40	324.6	123	0.34	0.12					
22 Larsen Inlet	807.9	-0.42	3.9	-2.8	-0.01	582.5	87.8	342	-0.85	-0.50	225.4	51	0.17	0.04					
23 D-B-E Gl.	822.7	-0.94	11.3	-2.2	-0.01	502.8	95.1	302	-1.91	-0.96	320.0	166	-0.23	-0.07					
24 Nordenskjöld Cst. 24a Fothergill 24b Arrol Icefld.	590.4 227.6 363.6	-0.73 0.07 -0.78	4.5 4.5	-3.1 -3.1	-0.01 -0.01	391.5 143.8 248.1	95.5 96.4 94.9	190 179 11	-2.14 0.41 -3.68	-0.84 0.06 -0.91	198.9 83.8 115.5	69 27 42	0.22 0.11 0.41	0.04 0.01 0.05					
25 Drygalski Gl.	963.4	-2.39	9.6	-2.2	0.01	618.0	69.1	760	-4.14	-2.56	345.4	43	-0.29	-0.10					
26 Seal Nunataks 26a Rogosh Gl. 26b Robertson Is.	665.3 491.7 173.6	-0.80 -0.56 -0.24	-- -- --	-- -- --	-- -- --	575.3 401.7 173.6	59.5 85.2 0.0	292 125 167	-1.52 -1.52 -1.54	-0.87 -0.60 -0.27	90.0 90.0 --	(4) (4) --	(-0.31) (-0.31) --	-0.02 -0.02 --					
27 Hektoria-Green Gl.	1146.2	-3.84	85.9	-12.4	-0.53	714.4	62.1	506	-5.05	-3.60	431.8	(18)	-0.31	-0.13					
28 Evans Gl.	299.1	-0.72	27.4	-2.8	-0.04	259.2	57.2	116	-2.92	-0.76	39.9	(1)	(-0.31)	-0.01					
29 Jorum-Punchbl. Gl.	596.8	-0.51	42.8	-3.8	-0.15	313.2	80.4	179	-1.93	-0.60	283.6	143	0.19	0.05					
30 Crane Gl.	1314.8	-2.24	50.4	-3.9	-0.10	409.3	60.1	430	-5.78	-2.36	905.5	318	0.03	0.03					
31 Cape Disappt. 31a M-M-P Gl. 31b Starbuck-Stubb Gl.	1098.5 662.4 435.3	-0.36 -0.23 -0.17	11.7 11.7	-1.1 -1.1	-0.00 -0.00	958.5 588.0 370.5	47.2 45.2 50.4	719 436 283	-0.45 -0.38 -0.56	-0.43 -0.23 -0.21	140.0 75.4 64.8	58 (9) 49	0.35 (-0.31) 0.36	0.05 -0.02 0.02					
32 Flask Gl.	1247.3	0.12	--	--	--	714.2	58.2	782	0.32	0.23	533.1	150	-0.19	-0.10					
33 Leppard Gl.	1841.9	-1.31	--	--	--	1005.1	36.6	900	-1.00	-1.00	836.8	416	-0.54	-0.45					

Abbreviations for place names : AP, Antarctic Peninsula; B., Bay; Cst., Coast; Disappt., Disappointment; Du., Dundee; D'U., D'Urville; Gl., Glacier(s); Is., Island; Icefld., Icefield; JRI, James Ross Island; M-M-P, Mapple-Melville-Pequod; Pen., Peninsula; Pied., Piedmont; Punchbl., Punchbowl. ISL-impacted basins in **bold**.

^aAssuming mean density of 900 kg/m³ for all dV/dt measurements. Errors for these values are 0.9 times the sum of errors for dV/dt for each row.

^bArea determined from additional ASTER, SPOT, and Landsat images, spanning 2000-2002 to 2009-2010.

^cRate of elevation loss measured just above area of grounded ice retreat.

^dVolume loss assumes floatation was reached midway between 2001 – 2010 (period of observations).

^ePercent area covered by differential DEM satellite stereo-image data.

^fIf <20 ICESat dH/dt measurements are available, the regional mean measured ICESat dH/dt (-0.31 m a⁻¹) or, for sub-basins, the main basin mean, is used.

^gHypsometric weighting for areas below 1000 m; weighted by number of ICESat measurements for areas above 1000 m.

^hErrors on dV/dt can be determined by: ±0.3 m a⁻¹ * area for regions ≤1000 m a.s.l (dDEM data) and ±0.15 ma⁻¹ * area for regions >100 m a.s.l

ⁱFor these regions, dH/dt was determined by ICESat only.

Table S3. Surface mass input and mass imbalance

To assess the mass input and estimated net imbalance of the glacier basins in the nAP, we calculated the total mass input provided by the RACMO-2 climate model for each of the basins and elevation bin regions. We used the mean surface mass balance (SMB) for the period 1979-2011.

Table S3. Comparison of total mass balance (dM/dt) and input surface mass (dM_i/dt), and resulting **imbalance ratio**. Units: Area, km²; dM/dt, Gt a⁻¹; Mean dh/dt, m a⁻¹; SMB, kg m⁻² a⁻¹, dM_i/dt, Gt a⁻¹

Region	Ice-Covered Area	Total dM/dt	Mean dh/dt	Mean SMB	Total dM _i /dt	Imbal. ratio	<1000 dh/dt	<1000 SMB	<1000 dM _i /dt	<1000 ratio	>1000 dh/dt	>1000 SMB	>1000 dM _i /dt	>1000 ratio
nAP <66°S, 1-33	34232.8	-24.9	-0.77	1543	54.2	-0.46	-1.00	1295	29.9	-0.70	-0.31	2104	23.1	-0.18
nAP West, 1-11	14338.2	-4.8	-0.33	2112	30.4	-0.15	-0.27	1964	17.7	-0.12	-0.59	2361	12.6	-0.17
nAP North, 12-14	3688.0	-2.4	-0.69	537	2.0	-1.20	-0.69	537	2.0	-1.15	(-0.31)	920	0.0	--
nAP East, 15-33	16207.5	-17.7	-1.20	1268	21.8	-0.81	-1.75	1007	10.5	-1.56	-0.10	1844	9.8	-0.06
1 Bigo-Barilari B.	1737.4	-1.37	-0.88	2623	4.6	-0.30	-0.88	2317	1.9	-0.38	-0.88	2903	2.6	-0.28
1a Cadman Gl.	309.6	-0.37	-1.32	2582	0.8	-0.46	-2.23	2515	0.26	-0.80	(-0.88)	2616	0.54	-0.30
2 Trooz-Lever Gl.	1497.7	0.50	0.38	2052	3.1	0.16	0.72	1937	1.5	0.34	-0.0	2179	1.5	0.0
3 Flandres B.	1123.7	-0.45	-0.44	1816	2.0	-0.23	-0.14	1622	0.65	-0.08	-0.61	1926	1.4	-0.28
4 Anvers Is.	2155.9	-0.33	-0.17	2510	5.4	-0.61	-0.16	2431	4.8	-0.06	(-0.31)	3309	0.63	-0.07
4a Rieke B.	83.3	-0.21	-2.71	2100	0.17	-1.24	-2.71	2100	0.17	-1.24	--	--	--	--
5 Andvord B.	1163.2	-0.19	-0.18	1668	1.94	-0.10	-0.06	1510	0.97	-0.06	-0.33	1868	0.97	-0.16
6 Brabant Is.	916.7	-0.43	-0.46	2135	1.96	-0.22	-0.61	2058	1.4	-0.26	(-0.31)	2348	0.57	-0.11
6a Rush Gl.	43.6	-0.07	-1.71	1977	0.09	-0.81	-2.64	1991	0.06	-1.20	(-0.31)	1951	0.03	-0.11
7 Charlotte B.	505.5	-0.50	-1.09	1536	0.78	-0.64	-1.57	1512	0.48	-0.94	(-0.31)	1576	0.30	-0.15
8 Cayley Gl.	1512.6	-0.75	-0.54	2139	3.24	-0.23	-0.81	1979	1.6	-0.28	-0.25	2321	1.6	-0.10
9 Wright Ice Pied.	1370.1	-1.22	-0.99	2518	3.45	-0.35	-1.35	2204	1.9	-0.54	-0.40	3015	1.6	-0.12
10 Charcot B.	800.9	-0.37	-0.51	2073	1.66	-0.22	0.14	1739	0.76	0.07	-1.30	2473	0.90	-0.47
11 West Trinity	1571.5	0.68	0.48	1418	2.23	0.30	0.63	1371	1.8	0.42	(-0.31)	1661	0.42	-0.15
12 Mott Snowfield	987.7	-1.12	-1.26	731	0.72	-1.56	-1.26	730	0.72	-1.55	(-0.31)	920	0.00	--
12a North Duse B.	242.9	-0.45	-2.02	777	0.19	-2.37	-2.04	774	0.19	-2.32	(-0.31)	920	0.00	--
13 Tabarin Pen.	363.9	-0.65	-1.98	543	0.20	-3.25	-1.98	543	0.20	-3.24	--	--	--	--
14 Joinville-Du.-D'U. Is.	2336.4	-0.53	-0.25	454	1.06	-0.50	-0.25	479	1.06	-0.50	--	--	--	--
15 Vega Is.	175.7	-0.25	-1.58	499	0.09	-2.78	-1.58	498	0.09	-2.78	--	--	--	--
16 Snow Hill Is.	312.5	-0.27	-0.96	525	0.16	-1.69	-0.96	525	0.16	-1.69	--	--	--	--
17 North JRI	524.6	-0.64	-1.35	648	0.34	-1.88	-2.00	609	0.24	-2.93	0.05	791	0.11	0.06
18 South JRI	568.5	-0.24	-0.46	793	0.45	-0.53	-0.78	757	0.28	-0.93	0.13	871	0.17	1.59
19 West JRI	707.7	-1.52	-2.29	635	0.45	-3.38	-2.56	620	0.39	-3.69	(-0.31)	816	0.07	0.26
20 East Trinity	1347.0	0.55	0.51	1326	1.79	0.31	0.67	1268	1.42	0.48	(-0.31)	1620	0.37	-0.15
21 Sjögren Gl.	1177.3	-1.15	-1.09	1496	1.76	-0.65	-1.64	1224	1.04	-1.21	0.34	2303	0.75	0.14
22 Larsen Inlet	807.9	-0.42	-0.57	1563	1.26	-0.33	-0.85	1160	0.68	-0.66	0.17	2611	0.59	0.06
23 D-B-E Gl.	822.7	-0.94	-1.25	1750	1.44	-0.65	-1.91	1352	0.68	-1.27	-0.23	2426	0.78	-0.08
24 Nordenskjöld Cst.	590.4	-0.73	-1.36	1560	0.92	-0.79	-2.14	1425	0.56	-1.54	0.22	1844	0.37	0.10
24a Fothergill	227.6	0.07	0.30	1643	0.37	0.19	0.41	1505	0.15	0.36	0.11	1908	0.16	0.06
24b Arrol Icefld.	363.6	-0.77	-2.37	1506	0.55	-1.40	-3.68	1377	0.13	-6.30	0.41	1799	0.21	0.21
25 Drygalski Gl.	963.4	-2.39	-2.76	1606	1.55	-1.54	-4.14	1507	0.93	-2.48	-0.29	1782	0.62	-0.15
26 Seal Nunataks	665.3	-0.80	-1.34	807	0.54	-0.52	-1.52	756	0.43	-1.82	(-0.31)	1124	0.10	-0.18
26a Rogosh Gl.	491.7	-0.56	-1.26	975	0.48	-1.17	-1.52	939	0.38	-1.42	(-0.31)	1124	0.10	-0.18
26b Robertson Is.	173.6	-0.24	-1.54	332	0.06	-4.00	-1.54	332	0.06	-4.05	--	--	--	--
27 Hektoria-Green Gl.	1146.2	-3.84	-3.38	1461	1.67	-2.37	-5.05	1346	0.96	-3.38	-0.63	1648	0.71	-0.34
28 Evans Gl.	299.1	-0.77	-2.57	1083	0.32	-2.41	-2.92	1025	0.27	-7.87	(-0.31)	1474	0.06	-0.15
29 Jorum-Punchbl. Gl.	596.8	-0.51	-0.92	1296	0.77	-0.66	-1.93	1076	0.34	-1.59	0.19	1559	0.44	0.10
30 Crane Gl.	1314.8	-2.10	-1.77	1676	2.20	-0.95	-5.78	1320	0.54	-3.93	0.03	1848	1.67	0.02
31 Cape Disappt.	1098.5	-0.36	-0.35	780	0.86	-0.42	-0.45	732	0.70	-0.55	0.35	1104	0.15	0.30
31a M-M-P Gl.	662.4	-0.23	0.38	816	0.54	-0.43	-0.38	771	0.45	-0.46	(-0.31)	1168	0.09	-0.02
31b Starbuck-Stubb Gl.	435.3	-0.17	-0.42	722	0.31	-0.55	-0.56	668	0.25	-0.76	0.36	1028	0.07	0.23
32 Flask Gl.	1247.3	0.12	0.10	1179	1.47	0.08	0.32	802	0.57	0.36	-0.19	1700	0.91	-0.10
33 Leppard Gl.	1841.9	-1.31	-0.78	1511	2.78	-0.47	-1.00	821	0.82	-1.10	-0.54	2351	1.97	-0.21

Abbreviations for place names: AP, Antarctic Peninsula; B., Bay; Cst., Coast; Disappt., Disappointment; Du., Dundee; D'U., D'Urville; Gl., Glacier(s); Is., Island; Icefld., Icefield; JRI, James Ross Island; M-M-P, Mapple-Melville-Pequod; Pen., Peninsula; Pied., Piedmont; Punchbl., Punchbowl. ISL-impacted basins in **bold** (rows).

^aAssuming mean density of 900 kg m⁻³ for all dV/dt measurements.

^bRate of elevation loss measured just above area of grounded ice retreat.

^cVolume loss assumes floatation was reached midway between 2001 – 2010 (period of observations).

^dPercent area covered by differential DEM satellite stereo-image data.

^eNumber of repeat-track point measurements used. If <10 ICESat dH/dt measurements are available, the regional mean ICESat dH/dt (-0.31 m a⁻¹) or, for sub-basins, the main basin mean, is used.

^fHypsometric weighting for areas below 1000 m; weighted by number of ICESat measurements for areas above 1000 m.

Section S3. Error and Bias Analysis

Comparison of ICESat and dDEM dh/dt measurements

By extracting dh/dt at the same location from both the ICESat repeat-track analysis (slope-corrected dh/dt_{ICESat}) and the difference DEM analysis (dh/dt_{dDEM}) we examined biases and potential errors in dh/dt (Table S3). The errors in the overall comparison are small relative to other likely errors (e.g., ICESat measurement accuracy, firn corrections, spatial/temporal sampling limitations). As shown in the table, there may be a slight underestimate of the thinning in the dDEMs below 1000 m asl, but temporal differences in dh/dt may also be a component (as indicated by the large differences between western and eastern basins).

Table S4. Comparison of mean dh/dt (co-located dDEM and ICESat data)

	dh/dt_{dDEM}	dh/dt_{ICESat}	Number of Data Points
All study region (<66°S)	-1.77 m a ⁻¹	-2.09 m a ⁻¹	6158
<1000 m elevation	-2.08 m a ⁻¹	-2.42 m a ⁻¹	5213
>1000 m elevation	-0.06 m a ⁻¹	-0.23 m a ⁻¹	945
Northern (<65°S)	-1.32 m a ⁻¹	-1.25 m a ⁻¹	3206
Southern (>65°S)	-2.25 m a ⁻¹	-3.00 m a ⁻¹	2952
Western basins ¹	-0.14 m a ⁻¹	-0.60 m a ⁻¹	1195
Eastern basins ²	-3.21 m a ⁻¹	-3.73 m a ⁻¹	2820

¹Basins 1 – 11 exclusive of 1a, 4a, and 6a, i.e., without areas of significant ice front retreat.

²Basins 19, 21-25, 27-30, i.e., glaciers draining into major ice shelf loss areas.

Crossover analysis of ICESat data: consistency and slope correction test

There are 7 ICESat reference track crossover data sets with dDEM data in the study area. We compared both the slope-corrected and uncorrected elevation change data with the dDEM data for these sites, and ascending versus descending track data. Mean difference between the methods with the correction applied ($dDEM - ICESat_{corr}$) was +0.05 m a⁻¹. Without correction ($dDEM - ICESat_{uncorr}$), the mean difference rose to +0.96 m a⁻¹. Mean ICESat crossover differences between the ascending and descending passes, with the cross-slope correction applied, was 1.28 m a⁻¹. For uncorrected data at crossovers, the error again rises to 1.96 m a⁻¹. Note that large temporal differences are present in the ICESat crossover sites, as well as between the crossover data and the dDEM data. Moreover, crossover areas are a single measurement sites, and not the average of many adjacent measurements. Nevertheless, the difference data show that the slope correction reduces the elevation change analysis differences by ~0.7 to 0.9 m a⁻¹ for the available sites.

Bias analysis of dDEMs

For each basin, the differences shown in Table S4 [$dh/dt_{dDEM} - dh/dt_{ICESat}$] can be compared to the median of dh/dt_{dDEM} on nunataks, where no elevation change is expected (e.g. 'null' test). If the two values are similar, then it implies that the vertical shift measured on the nunataks is a realistic estimate of the bias and thus should be used to correct dh/dt_{dDEM} in each basin. A subset of 9 basins for which the volume change below 1000 m showed the greatest sensitivity was examined to determine if this correction should be applied (Figure S2). If the bias found from ICESat and the bias found on nunataks were the same, the data points should align on the 1:1 line. For four basins, applying the nunatak correction would lead to dh/dt_{dDEM} in better agreement with dh/dt_{ICESat} . For five basins (those located in the red quadrants), the opposite holds.

We consider the test inconclusive, and suggest it highlights problems associated with dDEM results in the vicinity of nunataks because (i) they are often only coarsely mapped in the Antarctic Digital Database, (ii) significant ice loss may be occurring at their margins and may bias the null test, and (iii) possible variations in rates of elevation change through the study period for individual basins combined with slightly different survey periods for ICESat and dDEM. Examining the satellite imagery, several of the nunataks are noticeably more exposed through time as ice is thinning adjacent to the outcrop. This is also confirmed by the non-Gaussian distribution of the vertical offset on nunataks which are skewed by a large number of highly negative values (Figure S3). Thus, estimating the dDEM elevation bias on nunataks is not an obvious question given a ‘collar’ of declining ice elevation and it may explain why applying our test in Figure S2 did not consistently lead to a path towards improvements.

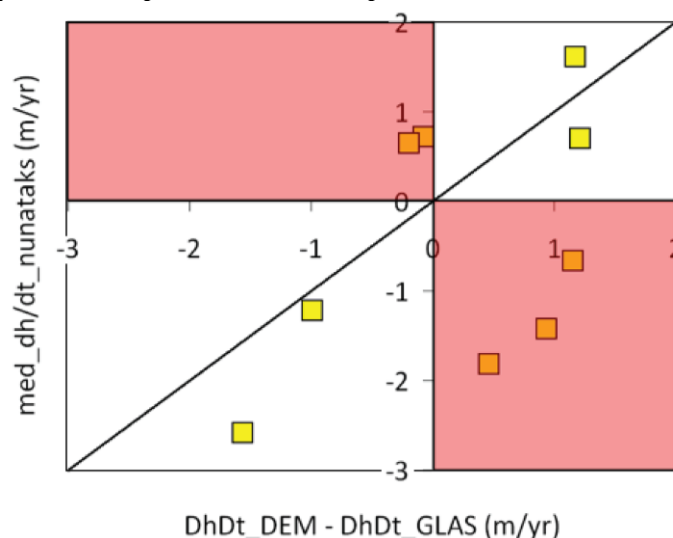


Figure S2: Analysis of dh/dt from the two methods for data near nunatak areas in high-mass-loss basins within the study area.

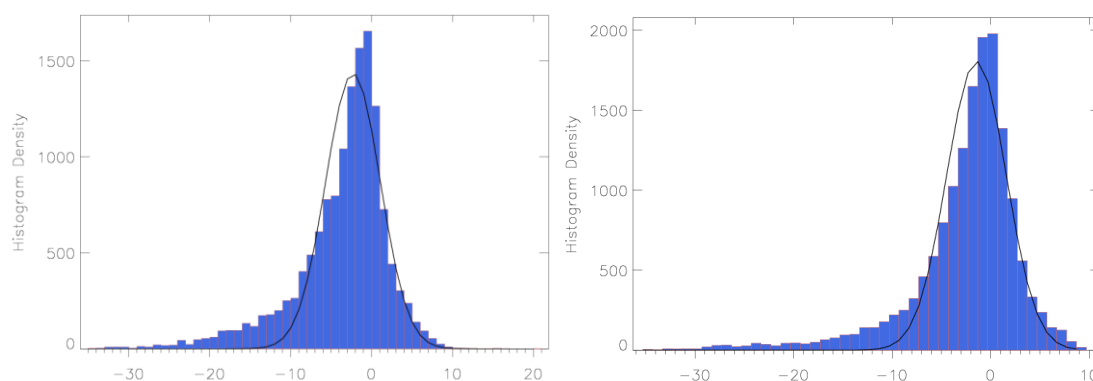


Figure S3. Distribution of elevation changes (in meters) over nunataks (as indicated in the ADD) for a test site near the Drygalski Gl. (Basin 25) and Hektoria-Green Gl. (Basin 27) drainage basins. The black line shows the best fit Gaussian curve for the distribution. The x-axis shows meters per year elevation change.

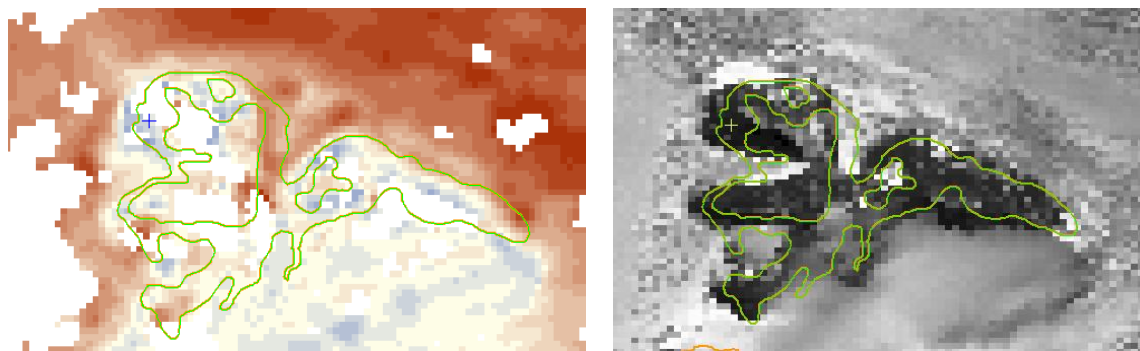


Figure S4. A large nunatak area in the dDEM image (left) and a single SPOT-5 image (right). Nunatak extent outline from the ADD is shown in green. The dimensions of the box are about 1 km by 0.5 km.

Overlaying the nunataks (from ADD) on the images and the dh/dt_{DEM} maps shows that nunataks are sometimes shifted with the images so that the nunatak outlines include rapidly thinning glacier areas. This explains the inclusion of some strongly negative dh/dt values in Fig. S3.

Section S5. References for Supplemental Information

Cook, A. J., Murray, T., Luckman, A., Vaughan, D. G., and Barrand, N. E.: A new 100-m Digital Elevation Model of the Antarctic Peninsula derived from ASTER Global DEM: methods and accuracy assessment, *Earth System Science Data*, 4, 129–142, doi:10.5194/essd-4-129-2012, 2012.

Korona, J., Berthier, E., Bernard, M., Rémy, F., and Thouvenot, E.: SPIRIT. SPOT 5 stereoscopic survey of Polar Ice: Reference Images and Topographies during the fourth International Polar Year (2007-2009), *ISPRS J. Photogramm.*, 64, 204–212, doi:10.1016/j.isprsjprs.2008.10.005, 2009.

Berthier, E. and Toutin, T.: SPOT5-HRS digital elevation models and the monitoring of glacier elevation changes in North-West Canada and South-East Alaska, *Remt. Sens. Environ.*, 112(5), 2443-2454, doi :10.1016/j.rse.2007.11.004, 2008.

Berthier, E., Scambos, T., and Shuman, C.: Mass loss of Larsen B tributary glaciers (Antarctic Peninsula) unabated since 2002, *Geophys. Res. Lett.* L13501, doi : 10.1029/2012GL051755, 2012.

Haran, T., Bohlander, J., Scambos, T., Painter, T., and Fahnestock, M.: MODIS Mosaic of Antarctica (MOA) Image Map. Boulder, Colorado USA: National Snow and Ice Data Center, digital media, doi :10.7265/N5ZK5DM5, 2005.

Lenaerts, J. T. M., M. R. den Broeke, W. J. Berg, E. Meijgaard, and P. Kuipers Munneke: A new, high-resolution surface mass balance map of Antarctica (1979–2010) based on regional atmospheric climate modeling, *Geophys. Res. Lett.* 39, L04501, doi :10.1029/2011GL050713, 2012.